al Kimiya: Jurnal Ilmu Kimia dan Terapan
p-ISSN: 2407-1897, e-ISSN: 2407-1927
Vol. 12, No. 1 (26-34), June 2025/Muharram 1447

ADSORPTIVE PERFORMANCE OF GELATIN-HEMATITE COMPOSITE SYNTHESIZED FROM IRON LATHE WASTE USING GUAVA LEAF EXTRACT FOR Pb(II) REMOVAL FROM AQUEOUS SOLUTIONS

LILIK MIFTAHUL KHOIROH[1], HIMMATUL BARROROH[1*], MOH TAUFIK[1], MOH ROYYANUDDIN[1], RAMADHANA FATAHILLAH AL AKBAR[1], NADA RIFQI AMALIYAH[1], AND ENY YULIANTI[1]

[1]Chemistry Department, Science and Technology Faculty, Universitas Islam Negeri Maulana Malik Ibrahim Malang, Gajayana No.50 Street, Malang, 65144, Indonesia

*Corresponding Author email: himmatul.b@kim.uin-malang.ac.id

Article Information

Received: Nov 25, 2024
Revised: Apr 17, 2025
Accepted: Jun 07, 2025
Published: Jun 30, 2025

DOI:
10.15575/ak.v12i1.40817

Keywords:
adsorption; adsorption kinetics; gelatin-hematite composite

Abstract

Hematite was successfully synthesized from iron lathe waste using guava leaf extract as a reducing agent. To enhance adsorption capacity, hematite was composited with gelatin, a polymer containing amide and carboxylate functional groups. The hematite-gelatin composite was employed as an adsorbent for Pb solutions. This study investigated the material's structure and the adsorbent's performance, including the composite's optimum dosage and contact time. Characterization techniques included XRD, FTIR, SEM-EDX, and AAS analyses. XRD analysis revealed that the hematite-gelatin composite exhibited a high degree of crystallinity. FTIR analysis of the guava leaf extract spectrum identified phenolic vibrational absorption with strong intensity at 3447 cm^{-1} (O-H stretching) and a weak C-H vibrational bond at 2928 cm^{-1}. An ester group (C=O) at 1726 cm^{-1} indicated the presence of tannin compounds. For the hematite-gelatin composite, a C-O absorption band was observed at 1075 cm^{-1}, along with Fe-O absorption bands at 430 and 519 cm^{-1}. The SEM results show that the gelatin-hematite composite has a hollow and layered surface. The EDX analysis results show that the material contains C, N, O, Pb, and Fe, which indicates that gelatin has interacted with Pb when it becomes a composite and has absorbed Pb at a level of 1.4% after adsorption. Performance evaluation of the hematite-gelatin composite demonstrated high adsorption efficiency for Pb solutions. The adsorbent exhibited a high adsorption capacity of 800 mg/g with an optimal adsorbent dosage of 15 ppm and an optimal contact time of 70 minutes. The adsorption kinetics of the hematite-gelatin composite followed a pseudo-first-order adsorption model.

INTRODUCTION

Lead (Pb) is a toxic heavy metal that poses serious health risks when it accumulates in the body, potentially causing functional disorders, abnormalities, or diseases [1]. Additionally, lead contamination adversely impacts water and soil environments. Due to its persistence and strong adsorption properties, lead is challenging to degrade and, in excessive concentrations, poses severe threats to ecosystems. Consequently, the treatment and management of wastewater are essential to minimize these risks. Adsorption is a widely recognized and effective method for addressing heavy metal pollution [2][3]. This process can significantly reduce heavy metal concentrations in wastewater, mitigating environmental pollution risks. Among the various adsorbent materials available, hematite has demonstrated considerable potential as an effective medium for removing lead from aqueous systems [4][5].

Iron lathe waste is a byproduct of the metal-turning process and contains not only Fe but also various heavy metals, including Cu, in significant concentrations [6]. Proper waste management is essential to reduce both its toxicity and volume. One approach to handling iron lathe waste is synthesizing it into hematite [7]. Previous studies have focused on synthesizing various of iron oxides, such as hematite, maghemite, magnetite, and goethite, achieving high-purity products. Transforming lathe waste into functional materials enhances its economic value and mitigates the risk of environmental pollution. The synthesis of hematite can be facilitated using plant extracts as reducing agents [8][9].

Using plant extracts as reducing agents offers an alternative that reduces the reliance on chemicals, produces environmentally friendly, non-toxic materials, and facilitates the formation of nanoparticles [10][11]. Among various plant extracts, guava leaf extract has been identified as a particularly effective reducing agent [12][13]. Research conducted by Biswal et al. [13] demonstrated that guava leaf extract can support the synthesis of hematite nanoparticles. This extract is abundant in tannins and flavonoids, which chelate iron ions to form complexes that subsequently precipitate [12]. Furthermore, Sornapudi & Srivastava [14] reported that guava leaf extract contains 150% more tannins than other common sources, such as moringa, apple, lemon, and vitex, underscoring its superior potential as a natural reducing agent [13].

Applying guava leaf extract in hematite synthesis presents several notable advantages, such as producing high-purity hematite in nanoparticle form [15]. As nanoparticles, hematite offers an increased surface area, thereby improving its performance as an adsorbent. Furthermore, hematite exhibits desirable characteristics, including selectivity, high adsorption capacity, and ease of separation due to its magnetic properties, facilitating efficient reuse [3]. Despite these advantages, using hematite as an adsorbent has certain limitations. Its surface stability is relatively low, as the adsorption process primarily relies on weak Van der Waals interactions. Additionally, hematite's low hydrophobicity hinders its dispersion in aqueous solutions. These challenges highlight the need for modifications to enhance its selectivity and effectiveness in binding metal ions in water [16].

A. Saad et al. [3] demonstrated that the chitosan-hematite composite forms an aggregated structure with a rough surface. This nanocomposite effectively reduces Pb and Cd concentrations, achieving a Pb adsorption capacity of 129.8 mg/g, although its capacity for Cu is relatively lower at 63.2 mg/g. This reduced efficiency is likely attributed to particle aggregation, leading to uneven surface ion adsorption. To overcome this limitation, chitosan can be substituted with gelatin. Research by Ulfa et al. [17] revealed that the gelatin-hematite composite exhibits a uniform hexagonal plate morphology with evenly distributed particles across the adsorbent surface. This structural uniformity enhances adsorption efficiency and improves the overall adsorption capacity.

Gelatin is a high-molecular-weight polypeptide that is water-soluble, non-toxic, biodegradable, and naturally sourced from animal derivatives such as skin, bones, and fish [18]. Its polymorphic molecular structure contains functional groups, including amino ($–NH_2$), hydroxyl (–OH), and carboxyl (–COOH), which contribute to its effectiveness as an adsorbent. NH_2 groups within the gelatin matrix allow it to adsorb metal ions in aqueous solutions through ion exchange facilitated by coordination bonds [3]. As a result, hematite composited with gelatin demonstrates high efficacy in adsorbing heavy metals from wastewater.

This study aims to synthesize gelatin-hematite composites from iron lathe waste, utilizing guava leaf extract as a reducing agent, to produce highly efficient nanoparticles in adsorbing metal ions. The resulting composite is expected to be environmentally friendly as a sustainable material that reduces environmental pollution. Additionally, this research seeks to address and repurpose waste materials effectively.

EXPERIMENT

Material

The materials utilized in this study included iron lathe waste, distilled or demineralized water, $Pb(NO_3)_2$ (p.a., Merck), HNO_3 (p.a., Merck), guava leaves, and gelatin (CDH).

Instrumentation

Instrumentation used in this research included X-Ray Diffraction (XRD) Philips Pt414241, Fourier Transform InfraRed (FTIR) 600 Series Agilent Technologies, Atomic Absorption Spectroscopy AAS

Procedure

Preparation of Precursors

A 50 g sample of separated iron lathe waste was placed into a 500 mL beaker, and 10 mL of 7 M HNO_3 was added. The mixture was left to stand at room temperature for 24 hours, after which it was filtered through filter paper to remove any impurities. The filtrate was then heated on a hot plate and stirred with a magnetic stirrer until a slurry formed.

Preparation of Guava Leaf Extract

The extraction of guava leaves using the infusion method consists of several stages. First, the freshly harvested guava leaves are thoroughly washed with running water and rinsed with distilled water. After air-drying, the leaves are ground into a fine powder. A portion of 40 g of ground leaves are weighed using an analytical balance, and each quantity is placed into separate 250 mL beakers. 100 mL of distilled water is added to each beaker, and the mixtures are stirred. The beakers are then placed in a water bath and heated at 80 °C for 30 minutes. After heating, the mixtures can settle, and the resulting solution is filtered through filter paper. The filtrate obtained is then used as a reducing agent.

Synthesis of Hematite-gelatin composite

Ten gs of precursor were added to 100 mL of distilled water, and 100 mL of guava leaf extract was added gradually, with continuous stirring using a magnetic stirrer. The mixture was then heated to 90°C for 1 hour while maintaining a stirring speed of 850 rpm, after which it was allowed to cool at room temperature for 24 hours. The resulting precipitate was decanted and washed with distilled water, filtered through a Buchner funnel, and air-dried at room temperature. The synthesized sample was subsequently calcined at 750 °C for 3 hours. In a separate procedure, 1 g of gelatin was dissolved in 100 mL of 1% acetic acid under stirring and then mixed with 5 g of hematite. This mixture was stirred until uniform and sonicated for 15 minutes [3].

Batch Adsorption

An adsorption experiment was conducted by introducing 10 mg of the gelatin–hematite composite into 50 mL of a 500 ppm $PbCl_2$ solution. The suspension was stirred at a constant speed of 200 rpm for 30 minutes to facilitate interaction between the adsorbent and Pb^{2+} ions. Upon completion of the contact time, the mixture was filtered, and the resulting filtrate was acidified using nitric acid (HNO_3). The residual lead concentration in the solution was then quantified using atomic absorption spectroscopy (AAS). To investigate the influence of adsorbent dosage on Pb^{2+} removal efficiency, the procedure was repeated with varying amounts of the gelatin–hematite composite: 5 mg, 15 mg, 20 mg, and 25 mg.

To evaluate the effect of contact time, the optimum dose of the adsorbent was mixed with 50 mL of a 500 ppm $PbCl_2$ solution. The mixture was agitated at 200 rpm for 10, 30, 50, 70, and 90 minutes. After each duration, a sample of the filtrate was acidified with HNO_3, and its absorbance was measured using an atomic absorption spectrometer (AAS).

Adsorption Analysis

Determination of removal Pb represented by (Equation 1-2) [19]:

$$\% \text{ Removal} = \frac{Co-Ce}{Co} \times 100\% \quad (1)$$

$$qe = \frac{(Co-Ce)\,V}{W} \quad (2)$$

Reaction Kinetics Study

The kinetics of the reaction were evaluated by applying pseudo-zero-order, pseudo-first-order, and pseudo-second-order models, as described by the following (Equations 3-6) [19]:

$$\frac{Ce}{qe} = \frac{1}{qo.b} + \frac{Ce}{qo} \quad (3)$$

$$\ln qe = \ln Kf + \frac{1}{n} \ln Ce \quad (4)$$

$$\ln (qe - qt) = \ln qe - k_1 t \quad (5)$$

$$\frac{t}{q_t} = \frac{1}{k_2(q_e)^2} - \frac{1}{q_e} t \quad (6)$$

Where qe is absorption capacity (mg/g), Co is initial concentration (mg/L), and Ce is equilibrium concentration (mg/L).

Reusable of gelatin-hematite composite for Pb

To evaluate the reusability of gelatin-hematite composite, 10 ppm $PbCl_2$ solution was interacted with the adsorbent at the best dosage and adsorption was carried out with the optimum time. The desorption process was carried out by adding 10 mL of 0.01 M Na_2EDTA solution, followed by continuous stirring for 60 minutes. The adsorption-desorption cycle was repeated four times to assess the stability and regeneration ability of the composite material.

RESULT AND DISCUSSION

Characterization of Composite

The diffractogram of the synthesized hematite displays peaks that align with the standard hematite patterns (JCPDS database no. 33-0664), indicating a very high degree of crystallinity. However, after the synthesis with gelatin, a noticeable change was observed: the peak intensity decreased, and the peaks became somewhat broader, suggesting a reduction in crystallinity. This alteration can be attributed to the interaction with gelatin, which has semicrystalline characteristics [20]. As a result (**Figure 1**), the change in hematite's crystallinity was insignificant. Furthermore, the relatively small amount of gelatin used in the composite likely contributed to the minimal changes observed in the crystallinity and the diffractogram pattern of hematite.

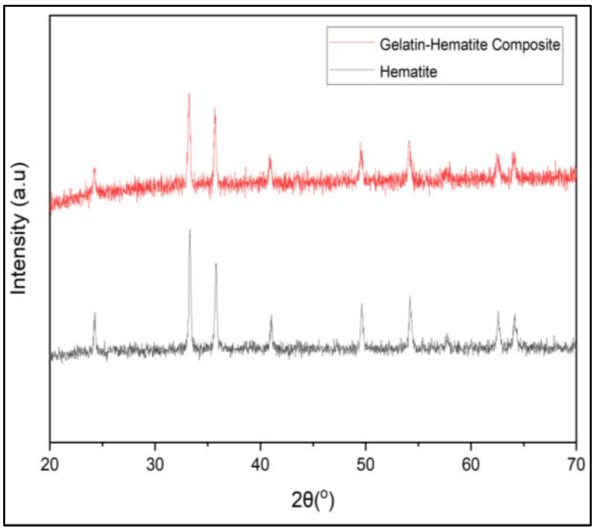

Figure 1. Diffractogram patterns of hematite and hematite-gelatin composite products.

The formation of hematite proceeds through a series of steps, beginning with the chelation of Fe^{3+} ions by tannin molecules to form a iron–tannin complex. Within this complex, Fe^{3+} ions are subsequently reduced to Fe^0, facilitating the generation of iron oxide nanoparticles. These nanoparticles then undergo phase transformation into hematite during the calcination process (**Figure 3**). The transformation of hematite is confirmed by data from FTIR (**Figure 2**).

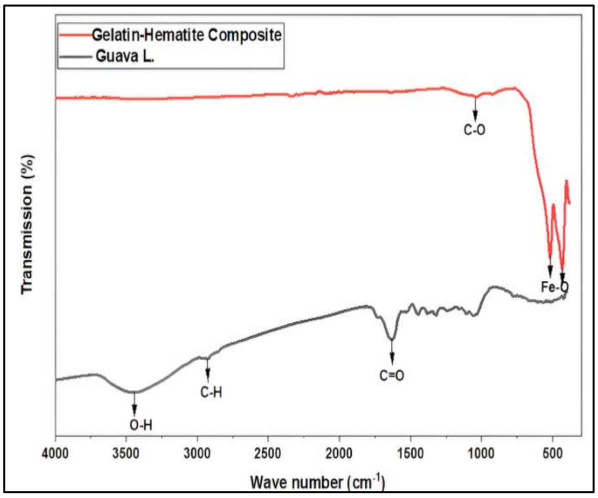

Figure 2. FTIR spectrum of guava leave extract and composite.

The spectrum of guava leaf extract shows a strong phenolic vibration absorption at 3447 cm^{-1}, corresponding to O-H stretching. A weak C-H vibration bond is observed at 2928 cm^{-1}. The presence of an ester group (C=O) at 1726 cm^{-1} indicates the existence of tannin compounds. In the gelatin-hematite composites, a C-O absorption is observed at 1075 cm^{-1}, while Fe-O group absorptions are detected at 430 cm^{-1} and 519 cm^{-1}.

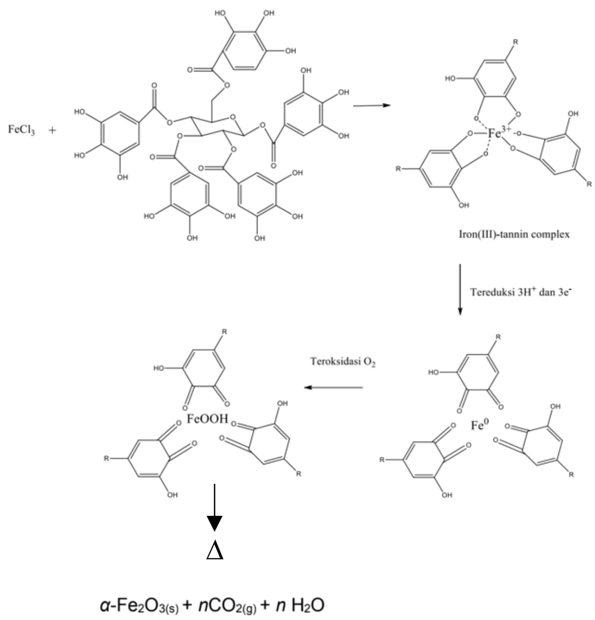

Figure 3. Mechanism of forming hematite [21] with modification.

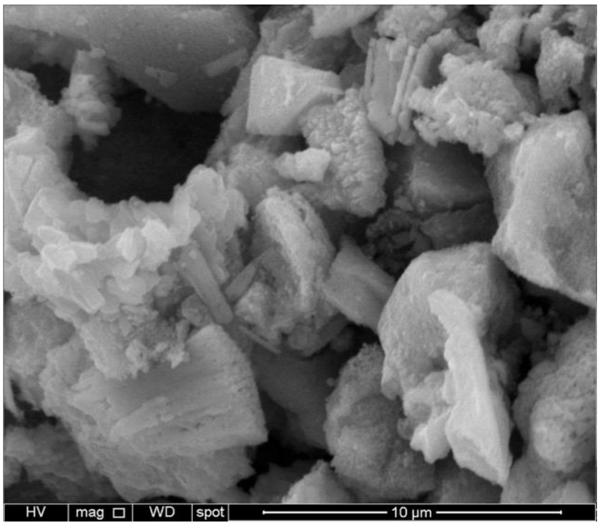

Figure 4. The Morphology of gelatin-hematite composite after Pb adsoprtion.

Based on the SEM results **(Figure 4)**, the gelatin-hematite composite exhibits hollow and layered morphology after adsorption. The presence of cavities within the composite facilitates the adsorption of Pb, leading to a notable decrease in its concentration in the solution. EDX analysis further reveals that the material has undergone an interaction between gelatin and hematite, as evidenced by the elemental composition: 2.6% carbon (C), 1.4% nitrogen (N), 18% oxygen (O), and 76.6% iron (Fe). Following the adsorption process, Pb is also found to be adsorbed within the cavities of the composite surface, indicated by a Pb content of 1.4% **(Figure 5)**. This demonstrates that the gelatin-hematite composite is effective in adsorbing Pb metal.

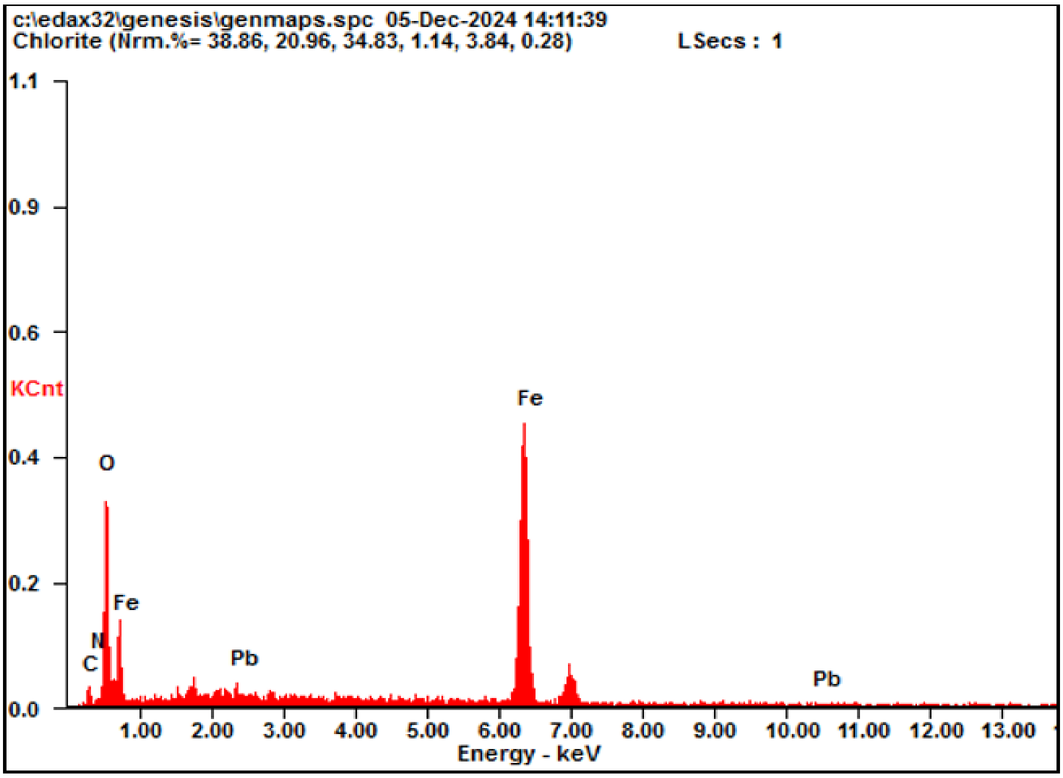

Figure 5. The EDX Spectrum of gelatin-hematite composite after adsorption.

Aplication of Hematite-Gelatin Composite for Adsorption of Pb Solution

The percentage of Pb removal following interaction with the adsorbent at doses of 15 mg and 20 mg reached approximately 82%, as illustrated in **Figure 6**. Although both doses yielded similar removal efficiencies, the 15 mg dose is considered optimal due to its more efficient use of adsorbent material. Utilizing a higher dose (20 mg) without a corresponding increase in removal efficiency indicates diminished adsorption effectiveness. At this optimal dose, Pb concentration was reduced most effectively. However, when the dose was increased to 30 mg, the removal percentage declined. This decrease may be attributed to the desorption of Pb ions from the composite surface at higher adsorbent loadings. Additionally, the lower removal efficiency at higher doses could be associated with excessive adsorbent mass, which may increase particle collisions and subsequently lead to the release of previously adsorbed Pb ions.

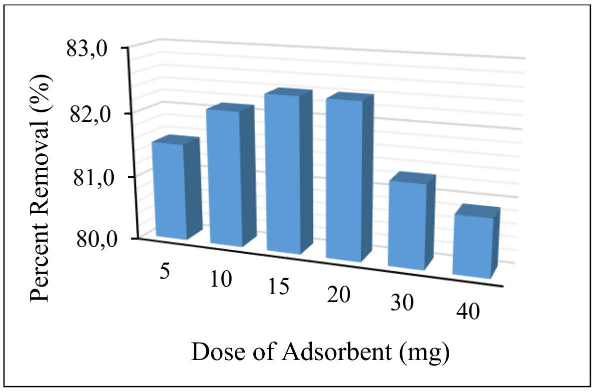

Figure 6. Percentage removal of Pb resulting from adsorption by hematite- gelatin composite.

The reduction in adsorption capacity with increasing adsorbent dose can be attributed to the formation of aggregates within the sample, where the adsorbent particles tend to cluster together. This aggregation reduces the surface area of the adsorbent, and as a result, the decreased surface area leads to lower adsorption efficiency **(Figure 7)**.

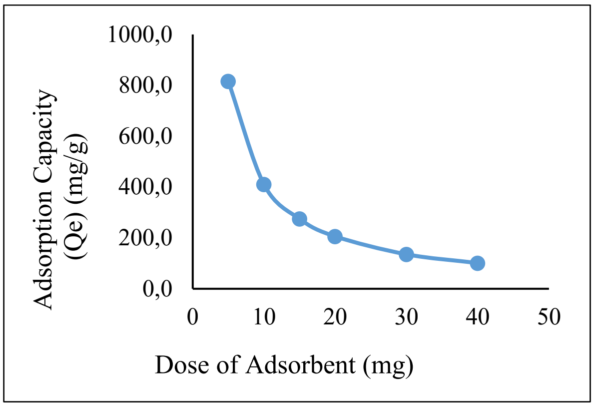

Figure 7. Pb adsorption capacity at various doses of gelatin-hematite composites.

Using the optimal dose and concentration, the adsorption process was carried out over different time intervals, including 10, 50, 70, 90, and 110 minutes. The results revealed that the optimal contact time for Pb adsorption was 70 minutes. After this time, the percentage of Pb removal declined, which can be explained by the saturation of the gelatin-hematite composite at 70 minutes **(Figure 8)**. Beyond this point, the active sites of the composite become unable to adsorb Pb effectively.

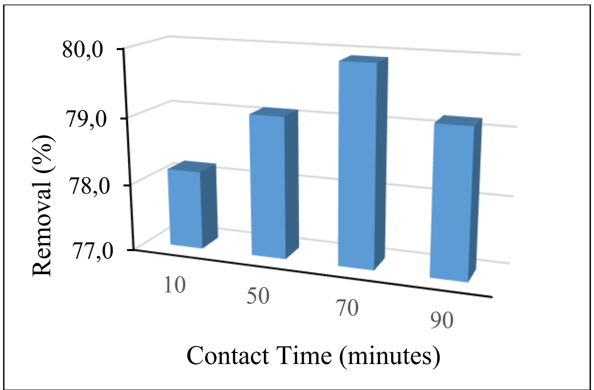

Figure 8. Percentage removal of Pb at various contact times.

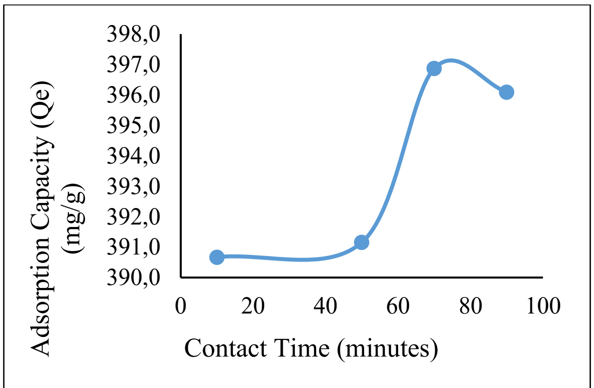

Figure 9. Relationship between adsorption capacity and contact time.

The adsorption capacity data regarding the effect of contact time demonstrate that the gelatin-hematite composite exhibits a very high adsorption capacity, reaching 397 mg/g **(Figure 9)**. This suggests that the adsorbent material has significant potential for absorbing Pb solution.

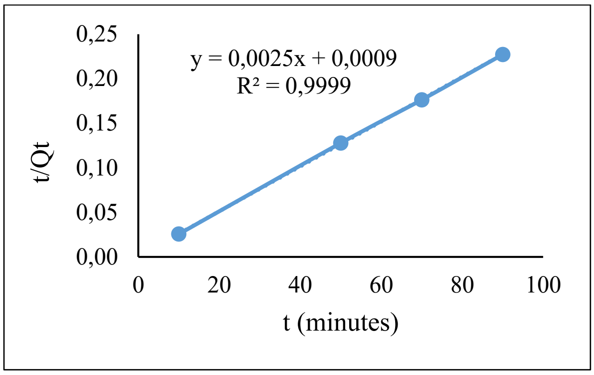

Figure 10. Pseudo-1st Order Kinetics.

The adsorption kinetic data indicate that the gelatin-hematite composite follows pseudo-first-order kinetics, as evidenced by the R-value approaching 1. This suggests that the adsorption process is primarily governed by a single kinetic mechanism, where the adsorption rate is influenced by the interaction between the adsorbate and the adsorbent surface rather than diffusion within the solution. Additionally, it can be inferred from this data that the rate of change in the concentration of adsorbed Pb is proportional to the amount of gelatin-hematite composite remaining in the solution **(Figure 10)**.

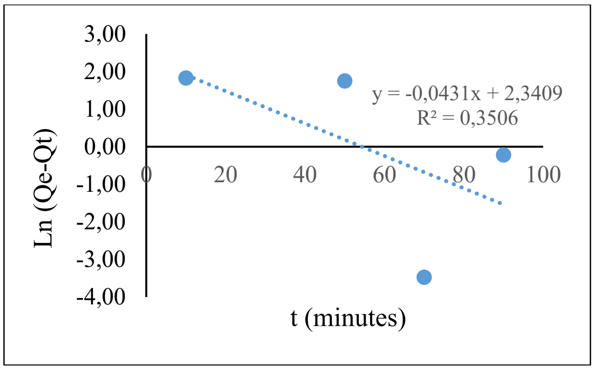

Figure 11. Pseudo 2nd Order Kinetics.

According **(Figure 11)**, the findings of this study indicate that the adsorption process does not follow pseudo-second-order kinetics. This implies that the adsorption primarily takes place on the surface of the adsorbent rather than being governed by diffusion processes or deeper interactions between the adsorbent and the adsorbate.

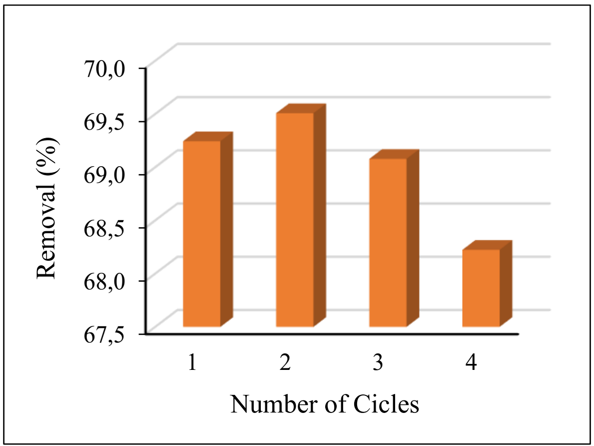

Figure 12. Regeneration of Hematite-Gelatin Composite for Removal Pb.

The regeneration process of the composite was performed over four consecutive cycles. The gelatin-hematite composite was utilized as a Pb adsorbent through four regeneration cycles. The results showed that the composite retained a high removal efficiency, reaching 69% after the fourth adsorption cycle. This highlights the potential of the gelatin-hematite composite as a reusable adsorbent, capable of sustaining significant removal efficiency over multiple regeneration cycles **(Figure 12)**.

CONCLUSION

The synthesized hematite-gelatin composite exhibits a high degree of crystallinity, with functional groups indicated by Fe-O stretching and amide absorption, thereby confirming a significant interaction between hematite and gelatin. This composite demonstrates a hollow layered morphology and showcases remarkable adsorption efficiency, achieving an adsorption capacity of 800 mg/g. The optimal conditions for Pb adsorption are an adsorbent dosage of 15 ppm, and a contact time of 70 minutes. Furthermore, the kinetics of the adsorption process conform to a pseudo-first-order model, suggesting a rapid adsorption mechanism. These findings indicate that the hematite-gelatin composite holds great promise as an effective material for removing Pb from aqueous solutions.

ACKNOWLEDGEMENT

The author acknowledges; Basic Research Study Program, Institute for Research and Community Service of Maulana Malik Ibrahim State Islamic University of Malang, and iron oxide team for the supporting of this research.

REFERENCES

[1] M. W. Syafriliansah and T. Purnomo, "kadar logam berat timbal (Pb) tumbuhan aquatik dan air sebagai indikator kualitas air sungai Brangkal Mojokerto", *LenteraBio : Berkala Ilmiah Biologi*, **11**(2), 341–350, 2022, https://doi.org/10.26740/lenterabio.v11n2.p341-350

[2] Z. Sihang, W. Shuai, Y. Xiao, T. Shah, C. Chong, W. Xiang, S. Jianying, "Green sustainable and highly efficient hematite nanoparticles modified biochar-clay granular composite for Cr(VI) removal and related mechanism", *Journal of Cleaner Production*, **276**, 2020, https://doi.org/10.1016/j.jclepro.2020.123009

[3] A. H. A. Saad, A. M. Azzam, S. T. El-Wakeel, B. B. Mostafa, and M. B. Abd El-latif, "Industrial wastewater remediation using Hematite@Chitosan nanocomposite", *Egyptian Journal of Aquatic Biology & Fisheries*, **24**,(1), 13–29, 2020, https://doi.org/10.21608/ejabf.2020.67580

[4] B. P. N. Gunawardhana et al., "Synthesis of hematite nanodiscs from natural laterites and investigating their adsorption capability of removing Ni^{2+} and Cd^{2+} ions from aqueous solutions", *Journal of Composites Science*, **4**(2), 2020, https://doi.org/10.3390/jcs4020057

[5] M. E. Mahmoud, M. M. Saleh, M. M. Zaki, and G. M. Nabil, "A sustainable nanocomposite for removal of heavy metals from water based on crosslinked sodium alginate with iron oxide waste material from steel industry", *Journal of Environmental Chemical Engineering*, **8**(4), 2020, https://doi.org/10.1016/j.jece.2020.104015

[6] L. M. Khoiroh, A. D. A. Sholekah, and E. Yulianti, "Structure and morphology properties of nanoparticle hematite pigment from lathe waste", *International Journal of Chemistry*, **13**(1), 2021, https://doi.org/10.5539/ijc.v13n1p21

[7] L. M. Khoiroh, M. N. Al-Chabib, and A. Prasetyo, "Synthesis and characterization of hematite (α-Fe_2O_3) from lathe waste using co-precipitation -calcination method", *IOP Conference Series: Materials Science and*

Engineering, **578**(1), 2019, https://doi.org/10.1088/1757-899X/578/1/012004

[8] A. Rufus, N. Sreeju, and D. Philip, "Size tunable biosynthesis and luminescence quenching of nanostructured hematite (α-Fe_2O_3) for catalytic degradation of organic pollutants", *Journal of Physics and Chemistry of Solids*, **124**, 221–234, 2019, https://doi.org/10.1016/j.jpcs.2018.09.026

[9] Md. S. H. Bhuiyan, M. Y. Miah, S. C. Paul, T. Das Aka, O. Saha, Md. M. Rahaman, Md. J. I. Sharif, O. Habiba and Md. Ashaduzzaman, "Green synthesis of iron oxide nanoparticle using Carica papaya leaf extract: application for photocatalytic degradation of remazol yellow RR dye and antibacterial activity", *Heliyon*, **6**(8), 2020, https://doi.org/10.1016/j.heliyon.2020.e04603

[10] R. R. Banala, V. B. Nagati, and P. R. Karnati, "Green synthesis and characterization of Carica papaya leaf extract coated silver nanoparticles through X-ray diffraction, electron microscopy and evaluation of bactericidal properties", *Saudi Journal of Biological Sciences*, **22**(5), 637–644, 2015, https://doi.org/10.1016/j.sjbs.2015.01.007

[11] C. M. Sangode, S. A. Mahant, P. C. Tidke, M. J. Umekar, and R. T. Lohiya, "Green synthesized of novel iron nanoparticles as promising antimicrobial agent: A review", *GSC Biological and Pharmaceutical Sciences*, **15**(2), 117–127, 2021, https://doi.org/10.30574/gscbps.2021.15.2.0130

[12] S. P. Patil and P. M. Rane, "Psidium guajava leaves assisted green synthesis of metallic nanoparticles: a review", *Beni-Suef University Journal of Basic and Applied Sciences*, **9**(1), 2020, https://doi.org/10.1186/s43088-020-00088-2

[13] S. K. Biswal, G. K. Panigrahi, and S. K. Sahoo, "Green synthesis of Fe_2O_3-Ag nanocomposite using Psidium guajava leaf extract: An eco-friendly and recyclable adsorbent for remediation of Cr(VI) from aqueous media", *Biophysical Chemistry*, **263**, 2020, https://doi.org/10.1016/j.bpc.2020.106392

[14] S. D. Sornapudi and M. Srivastava, "Quantitative estimation of phytochemicals in different leaf extracts", *The Pharma Innovation Journal*, **11**(9s), 125-128, 2022, [*online*], https://www.thepharmajournal.com/special-issue?year=2022&vol=11&issue=9S&ArticleId=15270

[15] L. M. Khoiroh, D. A. Nisa, and R. F. A. Akbar, "The structure of hematite pigment from lathe waste using guava leave extract by hydrothermal method", *IOP Conference Series: Earth and Environmental Science*, **1439**, 2025, https://doi.org/10.1088/1755-1315/1439/1/012006

[16] P. Xu, G. M. Zeng, D. L. Huang, C. L. Feng, S. Hu, M. H. Zhao, C. Lai, Z. Wei, C. Huang, G. X. Xie and Z. F. Liu, "Use of iron oxide nanomaterials in wastewater treatment: A review", *Science of The Total Environment*, **424**, 2012, https://doi.org/10.1016/j.scitotenv.2012.02.023

[17] M. Ulfa, D. Prasetyoko, H. Bahruji, and R. E. Nugraha, "Green synthesis of hexagonal hematite (α-Fe_2O_3) flakes using pluronic F127-gelatin template for adsorption and photodegradation of ibuprofen", *Materials*, **14**(22), 2021, https://doi.org/10.3390/ma14226779

[18] C. V. T. Rigueto, M. T. Nazari, L. Á. Massuda, B. E. P. Ostwald, J. S. Piccin, and A. Dettmer, "Production and environmental applications of gelatin-based composite adsorbents for contaminants removal: a review *Environmental Chemistry Letters*, **19**(3), 2465–2486, 2021, https://doi.org/10.1007/s10311-021-01184-0

[19] D. Dimbo, M. Abewaa, E. Adino, A. Mengistu, T. Takele, A. Oro and M. Rangaraju, "Methylene blue adsorption from aqueous solution using activated carbon of spathodea campanulata", *Results in Engineering*, **21**, 2024, https://doi.org/10.1016/j.rineng.2024.101910

[20] N. Wang, J. Li, W. Lv, J. Feng, and W. Yan, "Synthesis of polyaniline/TiO_2 composite with excellent adsorption performance on acid red G," *RSC Advances*, **5**(27), 21132–

21141, 2015, https://doi.org/10.1039/C4RA16910G

[21] F. A. Shtewi, W. M. Barag and A. A. Tarroush, "Green Synthesis and Characterization of Iron Oxide Nanoparticles Using MenthaPiperita Leaves Extract", *International Science and Technology Journal*, **24,** 2021, [*online*], https://www.stcrs.com.ly/istj/en/article-details.php?id=312